FOLDABLE COMPOSITE STRUCTURES

J.C.H. Yee and S. Pellegrino[1]
Department of Engineering, University of Cambridge
Trumpington Street, Cambridge CB2 1PZ, UK

Abstract This paper presents a study of the folding of a new self-powered, self-latching tube hinge for deployable structures. This hinge is made by cutting three parallel slots in a thin-walled carbon fibre reinforced plastic (CFRP) tube, thus leaving three tape springs connecting the two ends of the tube.

Keywords: CFRP, deployable structures, tape springs

Introduction and Background

There is a growing trend in the aerospace industry towards simpler, cheaper and more reliable deployable structures. Hence, research is being carried out into structural concepts that can provide at the same time enhanced levels of functionality in comparison with previous designs for deployable booms, solar arrays, etc. and also require a smaller number of separate parts. One approach that is being pursued is to combine several functions in each structural element, and also to reduce the number and complexity of separate operations involved in constructing that element.

An example of this new approach is a self-powered, self-latching tube hinge made by cutting three parallel slots in a thin-walled carbon fibre reinforced plastic (CFRP) tube with circular cross-section. The slots divide the tube into three strips that are transversally curved; these strips —known as tape springs— can be flattened transversally and then bent longitudinally to form a localised fold, as shown in Figure 1. This structure is a replacement for a traditional pin-and-clevis hinge and is currently being considered for several space missions.

Tube hinges are designed such that their deformation during folding is entirely elastic. The uncut tube ends remain essentially undeformed, hence the deformation is almost entirely in the tape springs. The folding of a tube hinge can be simply described in terms of the inner tape springs deforming in *opposite sense bending* and the two outer tape springs deforming in *equal sense bending*. Here equal sense bending indicates that the bent tape spring has the same convexity as the straight one, see Fig. 2(a); in this case the edges of the tape spring are under compression. Conversely, opposite-sense bending indicates that the bent tape spring has opposite convexity to the bent one, Fig. 2(b), in which case the edges of the tape spring are under tension.

[1]Corresponding author: pellegrino@eng.cam.ac.uk

Figure 1: CFRP tube hinge (unfolded, folded 110°, folded 180°).

When an initially straight tape spring is subject to gradually increasing equal and opposite end rotations, initially it takes a uniform longitudinally curved shape. Its moment-rotation relationship is linear for sufficiently small rotations. If the tape spring is subject to opposite-sense bending, as the end rotations are increased the tape spring suddenly snaps and forms an elastic fold that is approximately straight in the transverse direction and has approximately uniform longitudinal curvature, Fig. 2(b). Then, if the rotations are further increased, the arc-length of the fold increases while its curvature remains constant. If, however, the tape spring is subject to equal-sense

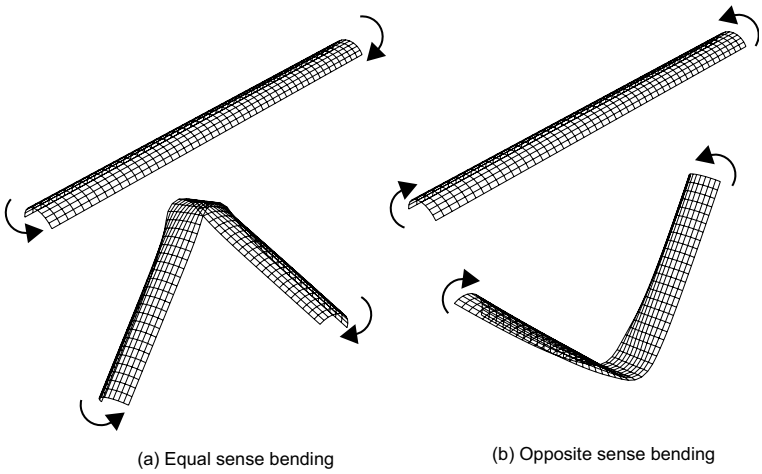

Figure 2: Two different ways of folding a tape spring.

bending, it deforms by gradually twisting over two adjacent, but separate regions whose lengths grow until the two folds merge into a single, localised fold, Fig. 2(a). Once this single fold has formed, further increasing the end rotation results —again— only in an increase of the arc-length of the fold region.

A folded tape spring has a natural tendency to deploy, thus resuming its straight configuration, and the combination of three tape springs in a tube hinge has the effect of increasing the deployment moment of the hinge, as well as increasing the moment that the hinge can resist without folding.

Tape springs made of isotropic materials (typically beryllium-copper or steel) have

been used for many years (Rimrott 1965). Rimrott (1970) and later Calladine (1988) have proposed an analytical model for predicting the longitudinal radius, r, of the uniformly curved region at the centre of an isotropic, folded tape spring with transverse radius of curvature R. An extension of this model to orthotropic shells of thickness t by Yee and Pellegrino (2003a) gives

$$r = \sqrt{\frac{D_{11}}{D_{22}}} R \tag{1}$$

where D_{11}, D_{22} are the bending stiffnesses of the shell in the longitudinal and transverse directions, respectively. This result is valid for both equal- and opposite-sense bending of the tape spring. The longitudinal strain in this curved region can be estimated from

$$\epsilon_x = \pm \sqrt{\frac{D_{22}}{D_{11}}} \frac{t}{2R} \tag{2}$$

where the sign is + for equal-sense bending and $z = +t/2$, or for opposite-sense and $z = -t/2$; the sign is − for equal-sense bending and $z = -t/2$, or for opposite-sense and $z = +t/2$. And the transverse strain from

$$\epsilon_y = \mp \frac{t}{2R} \tag{3}$$

where the sign is − at $z = +t/2$ and + at $z = -t/2$, regardless of the sense of bending.

This paper considers a particular tube hinge design, which requires the tape springs to fold so tightly that they have to operate close to failure. For this design, the paper presents a finite element analysis of the peak strains induced by the folding process. The geometric and material properties of the hinge are presented in the next section. Then a series of finite-element simulations of the folding of a single tape spring and of a tube hinge. The predictions obtained from the simulations are compared with predictions from Equations 1, 2 and 3 in the section Results. A Discussion concludes the paper.

Geometrical and Material Properties

The tube hinges considered in this paper are 82 mm long and have a circular cross-section with radius $R = 6.5$ mm. They are made from woven T300/913 prepregs (913C-814-40%, produced by Hexcel, which have 60% fibre content). The material properties of this prepreg are given in Table 1. In the central section there are three 50 mm long tape springs, each subtending an angle of 70°, which leaves 50° for each slot. The slots are machined with a radius of 3 mm at both ends.

One-ply and two-ply laminates are considered, corresponding to tube thicknesses of 0.27 mm and 0.47 mm. Yee and Pellegrino (2003b) have found that when T300/913 [0,90] laminates are folded in a direction that is perpendicular to one set of fibres and parallel to the other set, a one-ply laminate fails when it is subjected to a peak bending strain of about 2.7% in the direction of the fibres, whereas the two-ply laminate fails

at a bending strain of about 2.0%. On the other hand, when they are folded at 45° to the fibres, these laminates fail at peak strains around 5%, the corresponding fibre strains being around 2.5%. On this basis, it will be assumed that a one-ply tube hinge can survive bending strains along the fibres of up to 2.5% whereas for a two-ply hinge the bending strain limit is 2.0 %.

Table 1: Properties of 913C-814-40% prepregs

Elastic Moduli, $E_{11} \approx E_{22}$ (GPa)	46.0
Shear Modulus, G_{12} (GPa)	4.5
Poisson's ratio, $\nu_{12} = \nu_{21}$	0.065

Simulation of Folding Process

Detailed simulations of the folding of a single tape spring and of a complete tube hinge, consisting of three identical tape springs, were carried out with the ABAQUS (2001)package. Both one-ply and two-ply tape springs were analysed, and the linear-elastic material properties presented in Table 1 were assumed.

These simulations allow us to compare the deformation of a single tape spring with that of a hinge that is part of a tube hinge, so that we can better understand the structural behaviour of the actual tube hinge.

Element Choice

Since the interaction between bending and stretching stiffness of the tape springs plays an important role in determining the overall structural behaviour of a tube hinge, thin shell elements are clearly the most appropriate choice. ABAQUS offers several shell elements, and preliminary runs were carried out with 4-node quadrilateral full integration general purpose elements (S4); these elements have six degrees of freedom at each node. 4-node reduced integration shell elements (S4R5) with five degrees of freedom per node were also investigated. Eventually, the latter element was adopted, as it performs well for large rotations with only small strains. Furthermore, it uses reduced integration with hourglass control to prevent shear locking. It is also considered to be computationally economical and possesses high accuracy in modelling shell structures, as long as is not significantly distorted in plane. A typical mesh for a tape spring

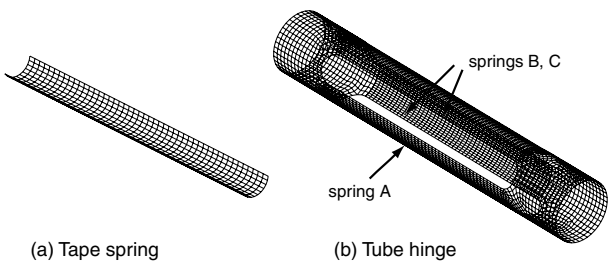

Figure 3: Typical FE models of tape spring and tube hinge.

involved 200 elements lengthwise by 30 elements widthwise. The mesh for a complete tape tube hinge had a similar mesh density and hence the number of elements was proportionally larger.

Simulation Techniques

The multiple point constraints (*MPC*) option was used to define the boundary conditions. For both the tape spring and the tube hinge models, the nodes on either end were tied to a *MPC* node, located at the centroid of the end cross section, through rigid beam elements. The main reason for locating the *MPC* nodes at the centroid is because the structure will be under pure bending when rotations are applied at the ends.

The three tape springs that constitute a tube hinge interact during the folding process, hence contact between these tape springs needs to be suitably modelled. ABAQUS defines the contact conditions between two bodies using a strict "master-slave" algorithm. The (*CONTACT PAIR) option needs to be specified for the two deformable surfaces, one of which is defined as the master surface and the other as the slave surface. In addition, the INTERACTION parameter is used to associate the contact pairs being defined with a surface interaction model, such as friction. The SMALL SLIDING parameter was chosen, instead of FINITE SLIDING, to achieve greater sensitivity to local initial gaps at the interface, caused by mismatch in the discretization of the meshed surfaces that come into contact. The SLIDING parameter sets up a slave node that interacts with the same region of the master surface throughout the analysis, despite the large displacements that occur during the simulation. The SURFACE BEHAVIOR parameter was set to the default, PRESSURE-OVERCLOSURE=HARD, which provides arbitrarily large contact forces as soon as the surfaces are in contact.

After having unsuccessfully attempted to use a default contact definition, a *symmetric* master-slave approach was adopted, i.e. two sets of contact pairs were defined for the same two surfaces, switching the roles of master and slave between the two tape springs. Despite involving additional computations, this approach provided improved convergence and accuracy.

A geometrically non-linear (*NLGEOM) incremental analysis was carried out using the Newton-Raphson solution method, with automatic stabilization provided through the STABILIZE function. This solution option automatically introduces pseudo-inertia and pseudo-viscous forces at all nodes when an instability is detected. Instead of continuing with the standard quasi-static analysis, ABAQUS automatically switches to a pseudo-dynamic integration of the equations of motion for the structure, thus avoiding numerical singularities. The pseudo viscous forces are calculated based on the model's response in the first increment of the analysis step, by assuming that the dissipated energy is a fraction of the strain energy during the first step. This fraction is known as *damping intensity*, which has a default value of 2×10^{-4}. To attain accurate results, it is desirable to set this parameter to the lowest value where convergence is still possible. In most of the analyses presented in this paper the damping intensity was set to 1×10^{-8}.

Results

This section presents the finite element analysis results for both the tape spring and the tube hinge, and compares the maximum strains and fold radii obtained from these detailed analyses with results from Equations 1-3.

Folding of Tape Spring

Figure 4 shows a series of snapshots from the folding sequence of a one-ply $[\pm 45^\circ]$ tape spring subject to opposite-sense bending under monotonically increasing end rotations of the two MPC nodes. The tape spring has radius $R = 6.5$ mm and subtends an angle $\theta = 130^\circ$.

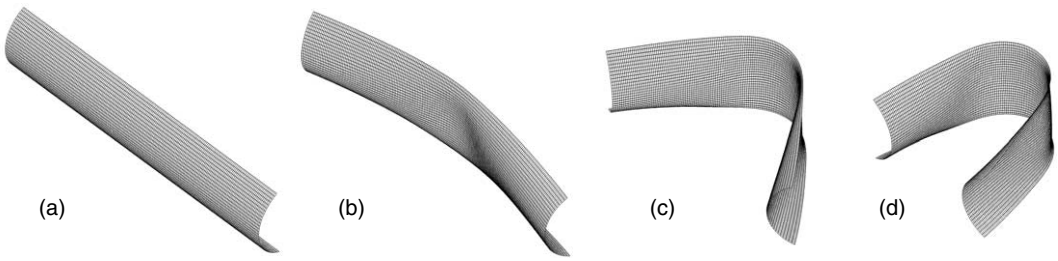

Figure 4: Folding sequence of tape spring subject to opposite-sense bending.

Figures 5, 6 shows contour plots of the principal strains, for opposite-sense and equal-sense bending of the tape spring. The strains on only one surface of the tape spring are shown, as the distribution on the opposite surface is practically identical, but with the sign reversed. This indicates that the mid-plane normal strains are negligibly small in this case. Note that both sets of strains are uniform through the central part of the tape spring, corresponding to the fold region, hence confirming that this region is uniformly curved.

Figure 7 shows contour plots of the strain distribution along the fibres at $+45^\circ$, for opposite-sense and equal-sense bending of the tape spring. The first thing to note in Figure 7 is that the largest strain, of around -2.3%, occurs when the tape spring is subject to opposite-sense bending. In the case of opposite-sense bending, Figure 7(a), fairly large tensile strains occur in two small regions on either side of the fold. There are only two such regions, not four, because we are considering the strain along one particular set of fibres. In the case of equal-sense bending, Figure 7(b), the strain in the central part of the fold region is quite small and so the largest strains occur in the small regions on either side of the fold. These peak localised strains are of the same magnitude as for the case of opposite-sense bending.

The characteristic tape-spring behaviour in which the strains localise around a uniformly curved region, requires that the angle θ subtended by the cross-section be sufficiently large to trigger this type of behaviour (as opposed to the standard bending

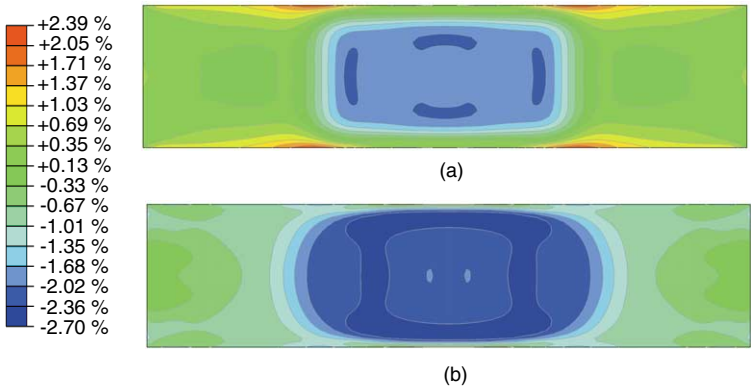

Figure 5: Principal strains on surface $z = +t/2$ of 1-ply $[\pm 45^\circ]$ tape spring under opposite-sense bending; (a) maximum principal strain; (b) minimum principal strain.

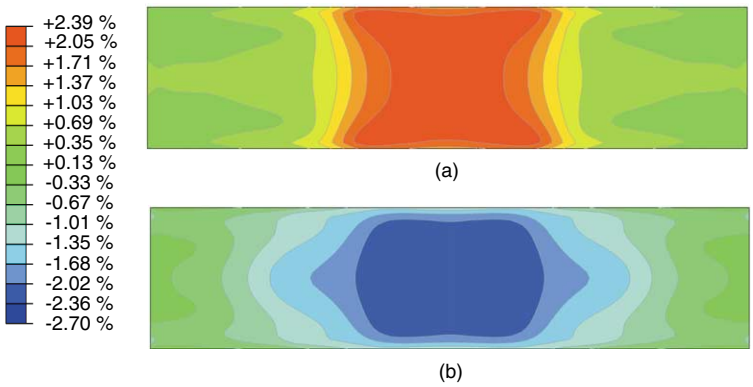

Figure 6: Principal strains on surface $z = +t/2$ of 1-ply $[\pm 45^\circ]$ tape spring under equal-sense bending; (a) maximum principal strain; (b) minimum principal strain.

of a plate). How large this angle needs to be depends on the interaction between out-of-plane bending and in-plane stretching, as well as on the degree of anisotropy of the tape spring. In the absence of a general, analytical expression for this limiting value of

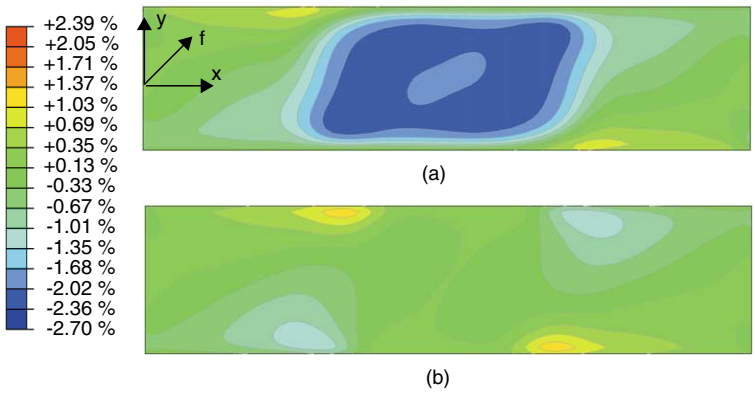

Figure 7: Strain along fibres at $+45°$, on surface $z = +t/2$ of 1-ply $[\pm 45°]$ tape spring for (a) opposite-sense bending and (b) equal-sense bending.

θ, a parametric study was carried out of the effects of gradually increasing θ in one-ply $[\pm 45°]$ and two-ply $[\pm 45°]_2$ tape springs. The study focussed on tape springs under opposite-sense bending but, once the critical value of θ had been identified, it was checked that this value would give satisfactory behaviour also for equal-sense bending. In all cases, a total rotation of 170° of one end of the tape spring with respect to the other was imposed.

The variation of the radius of curvature at the centre of the tape spring, and the peak tensile and compressive strains are presented in Table 2. Because θ does not appear in Eq. 1, the analytical prediction for r is 6.5 mm in all cases, as shown.

Table 2: Fold radii and maximum strains in tape springs

Laminate	Bending Mode	θ (deg)	r, Eq. 1 (mm)	r, FE (mm)	ϵ_f, FE (%)
1-ply	Opposite sense	70	6.50	9.27	-1.91, 1.77
$[\pm 45°]$		90	”	8.11	-2.01, 1.97
		110	”	7.35	-2.17, 2.10
		120	”	6.96	-2.27, 2.17
		130	”	6.52	-2.37, 2.25
	Equal sense	130	”	6.57	-1.26, 1.02
2-ply	Opposite sense	130	”	7.16	-3.78, 3.61
$[\pm 45°]_2$		140	”	6.65	-3.93, 3.73
		150	”	6.49	-4.10, 3.88
	Equal sense	150	”	6.53	-2.06, 1.68

Folding of Tube Hinge

Figure 8 shows four configurations of a one-ply $\pm 45^\circ$ tube hinge. In Fig. 8(a) the tube hinge is unstrained. In Fig. 8(b), corresponding to a relative rotation $\psi \approx 43^\circ$ between the two ends, a localised fold has formed in Spring A, which is under opposite-sense bending. Springs B and C are under equal-sense bending plus twisting; two localised folds have formed in each spring, but have yet to join up. The first contact between spring A and springs B and C occurs at $\psi \approx 79^\circ$, and they remain in contact from then on. Figure 8(c), corresponding to $\psi \approx 82^\circ$, shows a single localised fold in each tape spring. In Fig. 8(d), corresponding to a rotation $\psi \approx 170^\circ$, the end tubes almost come into contact. This can be avoided by adding two small, equal and opposite shear forces at the ends of the tube hinge, in addition to the pure moments applied throughout the folding process.

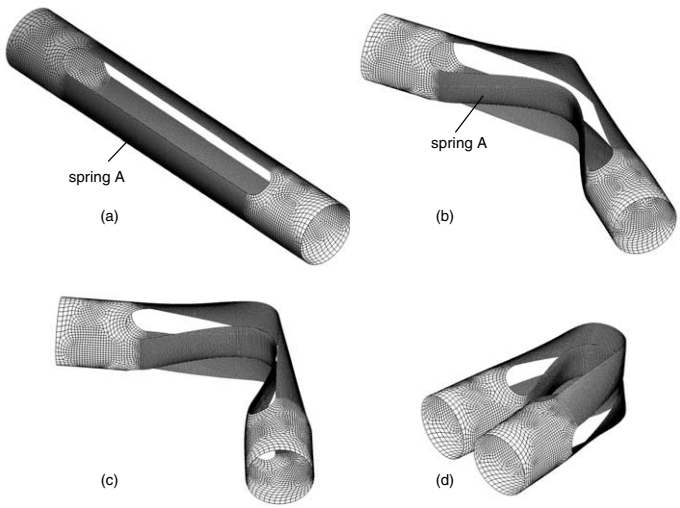

Figure 8: Folding sequence of tube hinge; (a) $\psi = 0^\circ$ (b) $\psi \approx 43^\circ$; (c) $\psi \approx 82^\circ$; (d) $\psi \approx 170^\circ$.

Figure 9 shows contour plots of the surface strains along the fibres at $+45^\circ$. The strain distribution in the outer surface of spring A, Fig. 9(a), is practically identical to that on the surface $+t/2$ of a tape spring on its own, Fig. 7(a). Also, the strain distribution on the inner surface of spring A, Fig. 9(b), is essentially equal and opposite to that in the outer surface. This indicates that, as for the case of a tape spring on its own, the mid-plane strains are again negligibly small.

Figure 9(c,d) shows contour plots of the surface strains on spring B; note that they are much smaller than in spring A. It is interesting to note that, because spring B has been twisted as well as bent, the regions of high localised fibre strains in Fig. 9(c,d) are both on the same edge of the tape spring, whereas in Fig. 7(b) they are on either edge.

The moment-rotation plot obtained from this simulation is shown in Fig. 10. Note

that the hinge behaves in a linear-elastic fashion for rotations $\psi < 3.7°$; at $\psi = 3.7°$ a limit point is reached and the corresponding moment is 852 Nmm. The tube hinge then gradually softens, reaching a minimum moment of ≈ 238 Nmm in the range $\psi = 77°$ to 104°. The moment remains approximately constant when ψ is further increased.

If the direction of ψ is reversed the hinge response is again initially linear, but this time springs B and C are under opposite-sense bending and so a higher limit moment is reached.

A comparison of the fibre strains predicted by the simple analytical model with finite-element predictions, using both the single tape-spring model and the complete hinge model, is presented in Table 3. Note that the analytical predictions of the largest fibre strain —which occur in the tape spring under opposite-sense bending— are underestimated by 10% to 15% when compared with the most accurate estimate, i.e. the complete hinge model.

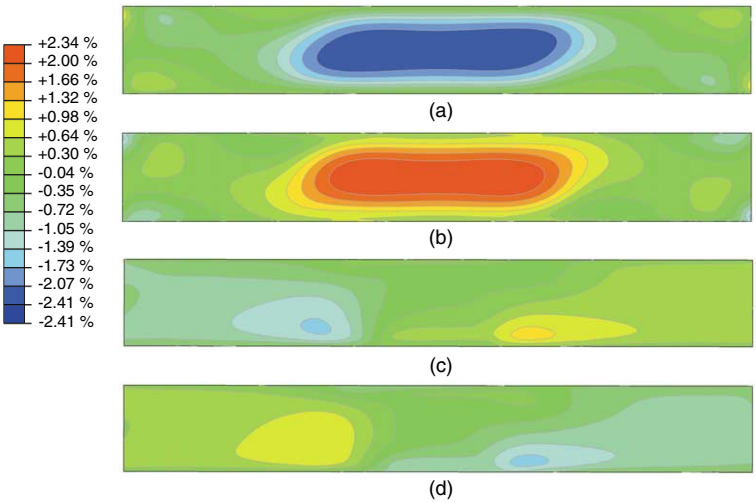

Figure 9: Strain along the fibres at +45° (%) for 1-ply [±45°] tube hinge. Spring A, (a) outer surface and (b) inner surface; spring B, (c) outer surface and (d) inner surface.

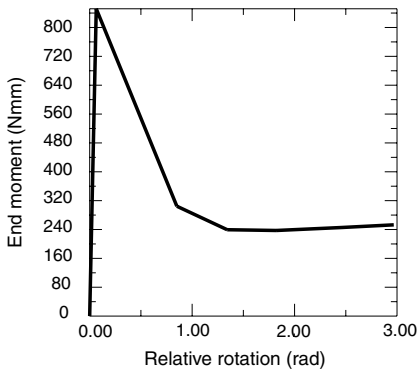

Figure 10: Moment-rotation relationship for tube hinge.

Table 3: Maximum strains along fibres in tube hinges

Laminate	Spring	Bending Mode	Location	Anal. (%)	FE tape spring (%)	FE tube hinge (%)
1-ply	A	Opposite sense	Outer	-2.08	-2.37	-2.41
$[\pm 45^\circ]$			Inner	2.08	2.25	2.34
	B, C	Equal sense	Outer	0.00	-1.26, 1.23	-1.20, 1.20
			Inner	0.00	1.02 -1.33	-1.27, 1.04
2-ply	A	Opposite sense	Outer	-3.62	-4.10	-3.72
$[\pm 45^\circ]_2$			Inner	3.62	3.88	3.31
	B, C	Equal sense	Outer	0.00	-2.06, 1.90	-1.58, 1.48
			Inner	0.00	-2.02, 1.68	-1.61, 1.48

Discussion and Conclusions

A detailed study of the deformation and strains induced by folding CFRP tape springs and tube hinges with a $\pm 45^\circ$ lay-up has been presented. This study has shown that the largest fibre strains in tape-springs under opposite-sense bending occur in the uniformly curved fold region and can be predicted with good accuracy using the analytical expressions obtained by Yee and Pellegrino (2003a). The same approach also gives accurate predictions for the maximum principal strains in tape-springs under equal-sense bending, which also occur in the uniformly curved fold region, however in this case the maximum fibre strains occur in small edge regions. For the two specific cases that have been analysed in detail it has been found that the maximum fibre strains were around 50% the maximum principal strain in the fold region.

A parametric study of the effects of varying the angle θ subtended by the cross-section has been conducted, showing that the longitudinal radius at the centre of a folded one-ply $[\pm 45^\circ]$ tape spring decreases by about 30% when θ is increased from 70° to 130°. It approaches a value close to the analytical estimate, both for opposite-sense and equal-sense bending. The two-ply $[\pm 45^\circ]_2$ tape spring also converges to the analytically estimated r, but at an even larger subtended angle $\theta = 150^\circ$. Clearly, the increased bending stiffness of the thicker laminate requires a larger subtended angle for the stretching-dominated behaviour to take over.

¿From a design viewpoint, the principal attraction of tape springs with larger θ's is that the they snap firmly into the straight configuration —a very attractive feature in the design of self-latching deployable structures—. Also, their peak strains are insensitive to the fold angle. However, tape springs with smaller θ's will generally have smaller strains for the same fold radius.

A complete tube hinge consisting of three tape springs has been investigated. This study has shown that contact between the tape springs occurs at fold angles of about 80°, but does not affect substantially the distribution and magnitude of the maximum fibre strains. A finite element analysis of a single tape spring provided, for both cases that have been considered, conservative estimates of the peak strains. These estimates

were particularly accurate for the single-ply tube hinge.

Turning to the specific tube hinge designs that were considered in this paper, it has been shown —in Table 3— that an 82 mm long tube hinge with cross-sectional radius of 6.5 mm and 50 mm long tape springs would be subject to a maximum fibre strain of -2.4% in the folded configuration, if it is made from a one-ply $[\pm 45]$, 0.27 mm thick 913C-814-40% prepreg. This strain is just within the limit of the material. A tube hinge made from a two-ply $[\pm 45]_2$ laminate, would be 0.47 mm thick and would be subject to maximum strains well in excess of the material limit. For this laminate to survive the folding process, the cross-sectional radius, or at least the radius of the tape spring that goes into opposite-sense bending should be increased.

Acknowledgements

The authors are grateful to Dr M.F. Sutcliffe for help and advice. Mr G.C. Dando and Dr A. Freeman, of QinetiQ Ltd., have provided sample tube hinges and have offered advice on many occasions. Mr J. Ellis, of Hexcel, Duxford, UK, has provided materials and manufacturing facilities. Financial support from Corpus Christi College, Cambridge and QinetiQ Ltd is gratefully acknowledged.

References

ABAQUS, Inc. (2001). ABAQUS Theory and Standard User's Manual, Version 6.2, Pawtucket, RI, USA.

Avery, W.B. (1998) Visilam 4: A laminate analysis spreadsheet, Boeing Corporation, Seattle.

Calladine, C.R. (1988) Love Centenary Lecture: The theory of thin shell structures 1888 - 1988. *The Institution of Mechanical Engineers Proceedings*, **202** (42):1-9.

Jones, R.M. (1999). *Mechanics of Composite Materials*, Second Edition. Taylor & Francis, Philadelphia.

Rimrott, F.P.J. (1965). Storable tubular extendible member: a unique machine element. *Machine Design*, **37**, 156-163.

Rimrott, F.P.J. (1970). Querschnittsverformung bei Torsion offener Profile. *ZAMM*, **50**, 775-778.

Yee, J.C.H. and Pellegrino, S. (2003a) CFRP tube hinges for deployable structures. Submitted for publication.

Yee, J.C.H. and Pellegrino, S. (2003b) Folding of composite structures. *Conference on Deformation and Fracture of Composites (FRC-7)*, Sheffield University, 22-24 April 2003.